©2016 March 25

Pade spectroscopy of structural correlation functions: application to liquid gallium[1]

N. M. Chtchelkatchev[a,b], B. A. Klumov[a,c,d], R. E. Ryltsev[a,e,f], R. M. Khusnutdinoff[a,g], A. V. Mokshin[a,g]

[a]Landau Institute for Theoretical Physics RAS, 142432 Chernogolovka, Russia

[b]Moscow Institute of Physics and Technology, 141700 Moscow, Russia

[c]Joint Institute for High Temperatures of the RAS, 125412 Moscow, Russia

[d]Aix-Marseille-Université, CNRS, Laboratoire PIIM, UMR 7345, 13397 Marseille, France

[e]Institute of Metallurgy UB of the RAS, 620016 Ekaterinburg, Russia

[f]Ural Federal University, 620002 Ekaterinburg, Russia

[g]Kazan (Volga Region) Federal University, 420008 Kazan, Russia

We propose the new method of fluid structure investigation which is based on numerical analytical continuation of structural correlation functions with Pade approximants. The method particularly allows extracting hidden structural features of non-ordered condensed matter systems from experimental diffraction data. The method has been applied to investigating the local order of liquid gallium which has non-trivial structure in both the liquid and solid states. Processing the correlation functions obtained from molecular dynamic simulations, we show the method proposed reveals non-trivial structural features of liquid gallium such as the spectrum of length-scales and the existence of different types of local clusters in the liquid.

Introduction. Gallium is a very specific metal [1]. First of all, it has enormously large domain of its phase diagram corresponding to liquid state. For example, the temperature interval of stable liquid state at ambient pressure is $(302.93, 2477)$ K. Diffraction experiments have shown that the local structure of liquid gallium is very complicated and it differs much from the local structure of typical simple liquids [2–5]. Accordingly, the crystal structure of gallium is also nontrivial: below its melting temperature $T_m = 302.93$ K at the ambient pressure the stable phase corresponds to the orthorhombic lattice which in nontypical for one-component metallic systems [6] (amount the other metals, the only Eu has the same lattice structure at ambient pressure). At higher pressures there is a lot of polymorphic transitions to other nontrivial crystal structures [7, 8].

Last time a lot of theoretical efforts were concentrated on investigation of the local structures and anomalies of gallium in liquid phase [9–12]. But there is a gap between theoretical investigations of gallium and experiment. The main problem is that the only

way to directly access the local structure is performing molecular dynamic (MD) simulations which can not unambiguously describe structure of real materials. Indeed, classical MD deals with model approximate potentials and first-principles MD has a problem of restricted spatial and time scales available in simulations. Experiment also can not directly access the local structure: the information about angle correlations is mostly lost in the static structure factor or radial distribution function (RDF); so only radial correlations can be extracted. Here, we develop a new method of correlation function processing based on complex analysis with Pade approximants.

Using this method we study local structure of liquid gallium and extract its non-trivial features. Analysing structural correlation functions obtained from MD simulations with EAM potentials, we extract the spectrum of spatial length scales and the existence of two types of local clusters. We show that the best fit of the gallium RDF can be performed using Lorentzians instead of Gaussians which are usually used for that purpose.

Local order of gallium. For MD simulations of liquid gallium, we have used LAMMPS molecular dynamics package. The system of $N = 20000-100000$ particles interacting via EAM potential [13], specially designed
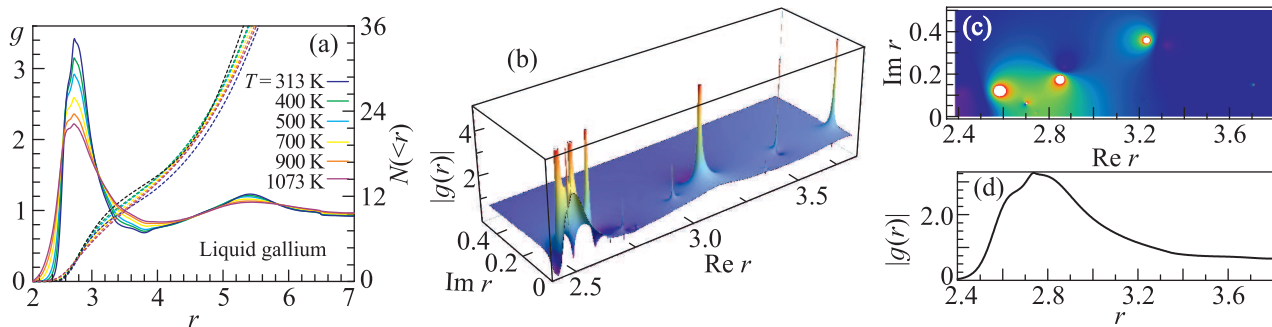

Fig. 1. (Color online) Pade spectroscopy of radial distribution function. (a) – Radial distribution function (RDF) $g(r)$ of liquid gallium (solid lines) and its distance-dependent co-ordination number $N(< r)$ (dashed lines) at different temperatures T (indicated on the plot). (b–d) – Liquid gallium, $T = 500$ K. (b) Doing the Pade approximation we find characteristic scales of gallium for particle distribution in the first coordination sphere: $r = 2.58, 2.69, 2.84$ Å. The scale $r = 3.33$ Å corresponds to the tail of the first coordination sphere. (c) – The density plot of the Pade approximant while. Panel d shows for comparison the first peak of $g(r)$

for gallium [14], was simulated under periodic boundary conditions in Nose–Hoover NPT ensemble. This amount of particles is enough to obtain satisfactory results. More simulation details can be found in Ref. [15] where similar simulation has been described. We checked that radial distribution functions obtained by our simulation quantitatively agree with those extracted from experiment [15].

Here, we focus on gallium at ambient pressure and investigate how its properties in liquid state depend on temperature. Fig. 1a shows the radial distribution function $g(r)$ of gallium taken for several temperatures in the range of $(313, 1073)$ K. The distance-dependent co-ordination number $N(< r) \equiv 4\pi\rho \int_0^r r'^2 g(r')dr'$, which is the mean number of particles inside a sphere of radius r, is also plotted in Fig. 1a; in part, the distance-dependent co-ordination number $N(< r)$ shows the number of nearest neighbors in the first coordination shell.

It is clear from the figure that the shape of the first RDF peak is nontrivial. It can be seen that the first RDF peak of gallium has clear shoulder. Particles forming the local clusters are mostly located at distances corresponding to the first coordination sphere (first peak of RDF). That suggests that local structure of liquid gallium is rather nontrivial. More detailed information can be extracted only after specific processing of RDF.

The promising way to extract features of local order hidden in RDF is performing analytical continuation to complex plane of distances. This is usual way in the theory of correlation functions of quantum systems especially for analytical continuation of the Greens functions from imaginary (Matsubara [16]) frequencies to the real frequency domain [17–19]. Recently the method

of numerical analytical continuation was successfully applied to investigations of velocity autocorrelation function of Lennard-Jones (LJ) fluid [20, 21] and in classical hydrodynamics of the Stokes waves [22]. Here we use this method for analysis of gallium RDFs. For numerical analytical continuation we build the Pade approximant [23, 24] like it was done in [17, 21]. More details we move into Supplementary Material [25].

The static structure factor is related to RDF as [26]:

$$S(k) = 1 + \frac{4\pi}{\rho} \, \text{Im} \int_0^\infty r[g(r) - 1]e^{ikr}dr. \qquad (1)$$

So, if $g(r)$ has a pole, at the position r_p, we should expect that the contribution of this pole to the structure factor oscillates like $\cos(k \, \text{Re} \, r_p)$ or $\sin(k \, \text{Re} \, r_p)$ and decays with k like $e^{-k \, \text{Im} \, r_p}$. Thus, knowledge of the poles gives important scales characterizing the particle system.

In Figs. 1b and c we show the results of the typical processing of gallium RDF by Pade approximants. As follows we use Pade approximant of RDF for its analytical continuation in complex-r. Fig. 1b shows the absolute value of RDF in complex-r plane while the peaks correspond to the poles. We see a limited number of poles near the real axis: so the Lorenzian fit of RDF perfectly matches all its basic features, see Figs.1c and d. The real parts of the positions of the poles are important length scales characterizing gallium: as follows, in the first coordination sphere: $r = 2.58, 2.69, 2.84$ Å; the scale $r = 3.33$ Å corresponds to the tail of the first coordination sphere. These scales are in fact characteristic interparticle distances in the first coordination shell. Thus we see that analytical continuation with Pade approximants allows extracting multi-scale character of lo-

cal structure of liquid gallium. In that connection, remember that, at ambient pressure, gallium crystallizes into non-trivial orthorhombic lattice and so it is interesting to find relation between unusual multiscale local order of the liquid and non-trivial crystal symmetry.

In Fig. 2 we show RDF obtained for ideal lattice of α-Ga (orthorhombic) with small random noise which
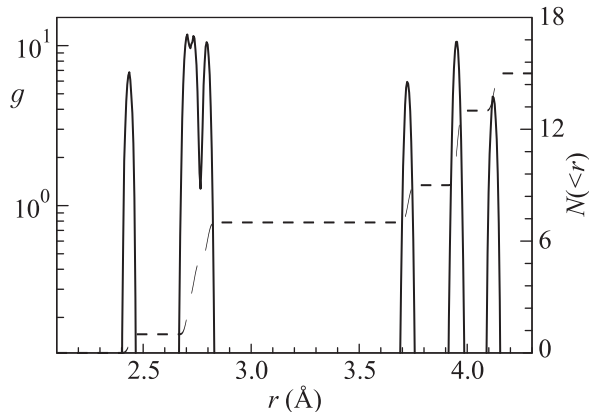

Fig. 2. RDF obtained for ideal lattice of α-Ga with small random noise which mimics thermal vibrations. The distance-dependent coordination number $N(< r)$ is also plotted by dashed line to evaluate the number of atoms at different shells

mimics thermal vibrations. We see that first coordination shell contains two atoms located at short distance of 2.46 Å. Such Ga_2 dimers were earlier suggested to be formed by covalent-like bonding [27]. Each Ga atom has another six nearest neighbour located in pairs in different coordination shells at distances 2.7, 2.73, 2.79 Å. So the crystal structure of α-Ga demonstrates spectrum of spatial scales. The comparison of these scales with those obtained from analytical continuation of RDF shows good agreement. Indeed the ratios of maximal and minimal distances are 1.134 for experimental lattice structure and 1.1 for scales extracted from liquid RDF. Of course the analytical continuation of liquid RDF does not distinct two nearly located scales. Recently, the similar analysis of liquid Ga structure was performed in [15] where simulated RDF were approximated by a set of Gaussians that gave similar interval of spatial scales. However, this methods can distinct only two scales in mentioned interval. Moreover the results strongly depend on the choice of approximation parameters such as the number and the shape of approximating functions [25].

For comparison we investigated LJ fluid and saw, unlike Gallium, two merging poles deep in the complex plain corresponding to the first peak of RDF. The poles show one characteristic scale – maximum of RDF [25].

Orientational order of Gallium. More detailed structural information can be obtained from analysis of orientational local order. The simplest way to describe it is calculating angular distribution function $P(\theta)$ which is probability density of angle θ between two vectors connecting a particle with its two nearest neighbors.

Fig. 3 shows bond angle distribution functions of liquid gallium at different temperatures T (indicated on the plot). Additionally the BADF of LJ-melt (which is nearly universal on the LJ melting curve) is also plotted for the comparison. Figs. 3b–d show BADF for $T = 500$ K. Looking at BADFs at real-θ axis, it is difficult to say something specific about the clusters forming the local order. But after its processing with the Pade approximant we see a number of poles in complex-θ plane. The positions of poles (Re θ) give characteristic angles between the particles forming the local order clusters. Particulary, we see two pronounced poles at the vicinity of the first peak which are located near the angles 45 and 60. The value of $\theta = 60$ is typical for simple liquids and corresponds to tetrahedral local order [28]. But the angle $\theta = 45$ suggests non-trivial symmetry of local clusters probably caused by the existence of short-bonded particles revealed by RDF analysis.

Another way to analyse orientational order is the well known bond order parameter method, which is widely used to characterize order in simple fluids, solids and glasses [29–33], hard spheres [34, 35], colloidal suspensions [36], complex plasmas [37–39], and metallic glasses [40].

Each particle i is connected via vectors (bonds) with its $N_{nn}(i)$ nearest neighbors (NN), and the rotational invariants (RIs) of rank l of second $q_l(i)$ and third $w_l(i)$ orders are calculated as:

$$q_l(i) = \left[\frac{4\pi}{2l+1} \sum_{m=-l}^{l} | q_{lm}(i)|^2 \right]^{1/2}, \qquad (2)$$

$$w_l(i) =$$
$$\sum_{\substack{m_1, m_2, m_3 \\ m_1+m_2+m_3=0}} \begin{bmatrix} l & l & l \\ m_1 & m_2 & m_3 \end{bmatrix} q_{lm_1}(i) q_{lm_2}(i) q_{lm_3}(i), (3)$$

where $q_{lm}(i) = N_{nn}(i)^{-1} \sum_{j=1}^{N_{nn}(i)} Y_{lm}(\mathbf{r}_{ij})$, Y_{lm} are the spherical harmonics and $\mathbf{r}_{ij} = \mathbf{r}_i - \mathbf{r}_j$ are vectors connecting centers of particles i and j. In Eq. (3), $\begin{bmatrix} l & l & l \\ m_1 & m_2 & m_3 \end{bmatrix}$ are the Wigner $3j$-symbols, and the summations performed over all the indexes $m_i = -l, ..., l$ satisfying the condition $m_1 + m_2 + m_3 = 0$. As shown in the pioneer paper [29], the bond order parameters q_l and w_l can be used as measures to charac-
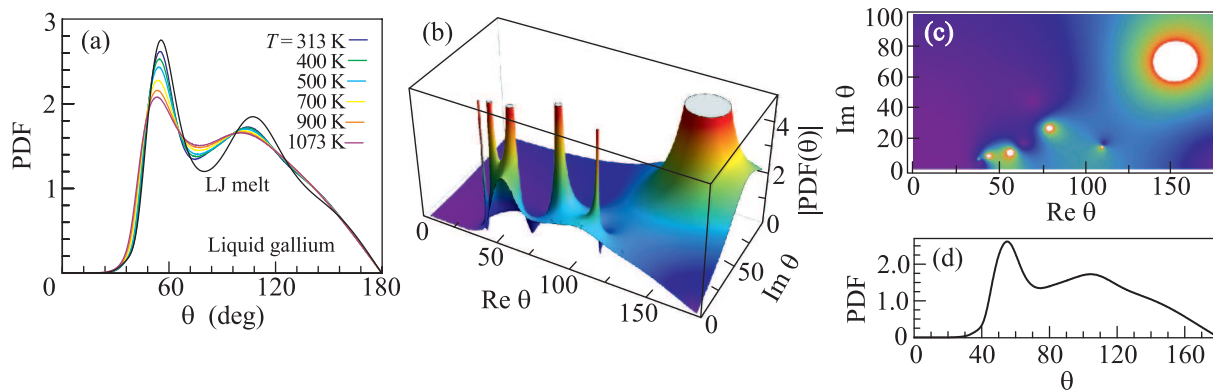
Fig. 3. (Color online) Pade spectroscopy of bond angle distribution function (BADF). (a) – BADF of liquid gallium at different temperatures T (indicated on the plot). Additionally the BADF of LJ melt (which is nearly universal on the LJ melting curve) is also plotted for the comparison. (b–d) – BADF for $T = 500$ K and its processing with Pade approximant. We see a number of poles, their positions ($\mathrm{Re}\,\theta$) give characteristic angles between the particles forming local order clusters
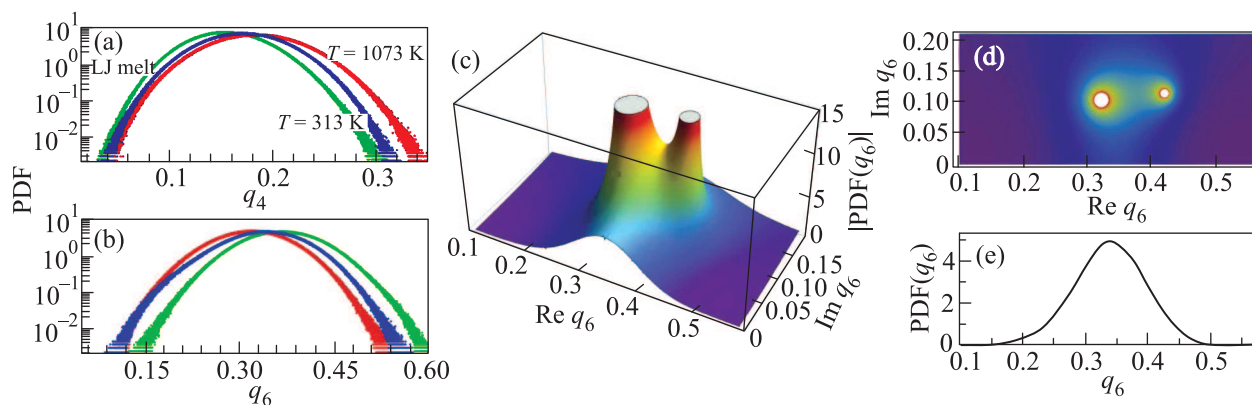

Fig. 4. (Color online) Pade spectroscopy of probability distribution functions (PDF). (a, b) – Orientational local order of liquid gallium: PDFs of the bond order parameters q_l ($l = 4, 6$) taken at two temperatures $T = 313$ K (blue line) and 1073 K (red line). Green solid lines represent the same PDFs for the LJ melt taken on the melting line (it can be shown that along the melting line these PDFs are practically universal). (c, d) – The absolute value of PDF ($l = 6$) of gallium for $T = 500$ K in complex q_6-plane. (e) – PDF of gallium for $T = 500$ K plotted for comparison with poles of the PADE-approximant in panel d. The poles are situated at $\mathrm{Re}\,q_6 = 0.32, 0.42$

terize the local orientational order and the phase state of considered systems.

Because each lattice type has a unique set of bond order parameters, the method of RIs can be also used to identify lattice and liquid structures in mixed systems. The values of q_l and w_l for a few common lattice types (including liquid-like Lennard-Jones melt) are presented in Table 1.

To quantify the local orientational order, it is also convenient to use the probability distribution functions (PDFs) $P(q_l)$ and $P(w_l)$. Fig. 4 shows the PDFs at different l ($l = 4, 6$) at different temperatures of liquid gallium in comparison to those calculated for LJ liquid [25, 28] whose PDFs are nearly universal along the melting line. We see again that such PDFs calculated at real-q_l axis (Figs. 4a and b) reveal no interest-

Table 1

Lattice type	q_4	q_6	w_4	w_6
hcp (12 NN)	0.097	0.485	0.134	-0.012
fcc (12 NN)	0.19	0.575	-0.159	-0.013
ico (12 NN)	$1.4 \cdot 10^{-4}$	0.663	-0.159	-0.169
bcc (8 NN)	0.5	0.628	-0.159	0.013
bcc (14 NN)	0.036	0.51	0.159	0.013
LJ melt (12 NN)	≈ 0.155	≈ 0.37	≈ -0.023	≈ -0.04

ing features of liquid gallium structure. We see broad dome-shaped distributions which are similar to those for LJ liquids [25]. But analytical continuation in the complex-q plane reveals that $P(q_l)$ are in fact composed of two Lorenzian-like peaks with similar values of both the maximum location ($\mathrm{Re}(q)$) and peak width ($\mathrm{Im}(q)$).

This fact suggests the structure of liquid gallium consists of two types of local order that is in agreement with the earlier obtained results [5, 11].

Conclusions. We propose the new method of fluid structure investigation which is based on numerical analytical continuation of structural data obtained from both experiment and computer simulations. The method particularly allows extracting hidden structural features of non-ordered condensed matter systems from experimental diffraction data. The method has been applied to investigating the local order of liquid gallium which is supposed to have complex structure. We show that analytical continuation of structural correlation functions such as radial distribution function, bond angle distribution function and bond orientational order parameters reveals non-trivial structural features of liquid. Firstly, we show that, processing the liquid RDF, our method allows easily obtaining the spectrum of length-scales which are in close agreement with those for crystal state. Secondly, we show for the first time that correlation functions of orientational order also have non-trivial features probably caused by the existence of different types of local clusters in the liquid.

---

1. Y. Waseda, *The Structure of Non-crystalline Materials: Liquids and Amorphous Solids*, McGraw-Hill, N.Y. (1980).

2. A. H. Narten, J. Chem. Phys. **56**, 5681 (1972).

3. Y. Waseda and K. Suzuki, Phys. Stat. Sol. B **49**, 339 (1972).

4. A. Lyapin, E. Gromnitskaya, O. Yagafarov, O. Stalgorova, and V. Brazhkin, JETP **107**, 818 (2008).

5. O. F. Yagafarov, Y. Katayama, V. V. Brazhkin, A. G. Lyapin, and H. Saitoh, Phys. Rev. B **86**, 174103 (2012).

6. A. F. Wells, *Structural Inorganic Chemistry*, Oxford University Press (2012).

7. O. Schulte and W. B. Holzapfel, Phys. Rev. B **55**, 8122 (1997).

8. T. Kenichi, K. Kazuaki, and A. Masao, Phys. Rev. B **58**, 2482 (1998).

9. S.-F. Tsay and S. Wang, Phys. Rev. B **50**, 108 (1994).

10. X. G. Gong, G. L. Chiarotti, M. Parrinello, and E. Tosatti, Europhys. Lett. **21**, 469 (1993).

11. J. Yang, J. S. Tse, and T. Iitaka, J. Chem. Phys. **135**, 044507 (2011).

12. K. H. Tsai, T.-M. Wu, and S.-F. Tsay, J. Chem. Phys. **132**, 034502 (2010).

13. D. K. Belashchenko, Physics-Uspekhi **56**, 1176 (2013).

14. D. Belashchenko, Russian J. Phys. Chem. A **86**, 779 (2012).

15. A. Mokshin, R. Khusnutdinoff, A. Novikov, N. Blagoveshensky, and A. Puchkov, JETP **148**, 947 (2015).

16. A. A. Abrikosov, L. P. Gorkov, and I. E. Dzyaloshinski, *Methods of Quantum Field Theory in Statistical Physics*, Courier Corporation (1975).

17. H. Vidberg and J. Serene, J. Low Temp. Phys. **29**, 179 (1977).

18. H. Yamada and K. Ikeda, Europ. Phys. J. B **87**, 1 (2014).

19. J. Schött, I. L. Locht, E. Lundin, O. Grånäs, O. Eriksson, and I. Marco, arXiv:1511.03496 (2015).

20. S. H. Krishnan and K. G. Ayappa, J. Chem. Phys. **118**, 690 (2003).

21. N. Chtchelkatchev and R. Ryltsev, Pis'ma v ZhETF **102**, 732 (2015).

22. S. Dyachenko, P. Lushnikov, and A. Korotkevich, JETP Lett. **98**, 675 (2014).

23. G. A. Baker and P. R. Graves-Morris, *Padé Approximants*, Cambridge University Press (1996), v. 59.

24. *Multipoint Padé Approximants*, Wolfram Mathworld.

25. See Supplemental material for this paper on JETP Letters suit: www.jetpletters.ac.ru.

26. J.-P. Hansen and I. R. McDonald, *Theory of Simple Liquids: With Applications to Soft Matter*, Academic Press (2013).

27. X. G. Gong, G. L. Chiarotti, M. Parrinello, and E. Tosatti, Phys. Rev. B **43**, 14277 (1991).

28. R. E. Ryltsev and N. M. Chtchelkatchev, Phys. Rev. E **88**, 052101 (2013).

29. P. J. Steinhardt, D. R. Nelson, and M. Ronchetti, Phys. Rev. B **28**, 784 (1983).

30. P. J. Steinhardt, D. R. Nelson, and M. Ronchetti, Phys. Rev. Lett. **47**, 1297 (1981).

31. J. R. Errington, J. Chem. Phys. **118**, 2256 (2003).

32. P. Rein ten Wolde, M. J. Ruiz-Montero, and D. Frenkel, J. Chem. Phys. **104** (1996).

33. B. Klumov, JETP Lett. **97**, 327 (2013).

34. M. D. Rintoul and S. Torquato, J. Chem. Phys. **105**, 9258 (1996).

35. B. A. Klumov, S. A. Khrapak, and G. E. Morfill, Phys. Rev. B **83**, 184105 (2011).

36. U. Gasser, E. R. Weeks, A. Schofield, P. N. Pusey, and D. A. Weitz, Science **292**, 258 (2001).

37. M. Rubin-Zuzic, G. E. Morfill, A. V. Ivlev, R. Pompl, B. A. Klumov, W. Bunk, H. M. Thomas, H. Rothermel, O. Havnes, and A. Fouquét, Nat. Phys. **2**, 181 (2006).

38. B. A. Klumov, Physics-Uspekhi **53**, 1053 (2010).

39. S. A. Khrapak, B. A. Klumov, P. Huber, V. I. Molotkov, A. M. Lipaev, V. N. Naumkin, H. M. Thomas, A. V. Ivlev, G. E. Morfill, O. F. Petrov, V. E. Fortov, Y. Malentschenko, and S. Volkov, Phys. Rev. Lett. **106**, 205001 (2011).

40. A. Hirata, L. J. Kang, T. Fujita, B. Klumov, K. Matsue, M. Kotani, A. R. Yavari, and M. W. Chen, Science **341**, 376 (2013).